J|A|C|S COMMUNICATIONS

Published on Web 09/16/2009

Double Metallocene Nanowires

Xiaojun Wu and Xiao Cheng Zeng*

Department of Chemistry and Nebraska Center for Materials and Nanoscience, University of Nebraska, Lincoln, Nebraska 68588

Received June 16, 2009; E-mail: xczeng@phase2.unl.edu

Organometallic multidecker sandwich clusters and nanowires have attracted increasing research attention because of their novel structural, electronic, magnetic, and transport properties.[1−31] Similar to the well-known ferrocene [$FeCp_2$] (Cp, C_5H_5),[1] a number of multidecker sandwich complexes can be highly stable, for example, TM_nBz_{n+1} (TM = transition metal, Bz = C_6H_6) and TM_nCp_{n+1} complexes, as well as the lanthanide rare earth metal−C_8H_8 complexes.[3−21] Also, quintuple-decker $V_n(BZ)_{n+1}$ clusters have been synthesized successfully and exhibit an intriguing ferromagnetic property.[3] Subsequent theoretical studies have shown a possible structural transition from achiral D_{6h} to chiral D_2 symmetry in these clusters, and the clusters' magnetic moments increase linearly with size n.[9−17] Considerable theoretical effort has also been devoted to the one-dimensional (1D) sandwich nanowires, including $[TMBz]_\infty$, $[TMCp]_\infty$, and $[TMAnt]_\infty$ (Ant = anthracene, $C_{12}H_{10}$), as well as the hybrid nanowires structures.[22−31] Some nanowires show novel magnetic, electrical transport, or half-metallic properties. As a result, metallocene clusters and nanowires can offer prototypes for molecular-based ferromagnet and spintronic devices, which may be exploited for applications in high-density information storage and quantum computing.

A pentalene (Pn = C_8H_6) is a polycylic hydrocarbon composed of two fused cyclopentadiene rings. Like Cp and Bz ligands, the pentalenes can encompass metal centers between two Pn planes. Since two metal atoms can be sandwiched between two Pn ligands, Pn−metal complexes are bimetallic analogues to the metallocenes. Katz et al. were the first to synthesize pentalene sandwich clusters Pn_2M_2 (M = Co and Ni). They observed diamagnetic properties, in contrast to the paramagnetic behavior in the bis(cyclopentadienyl) forms.[32,33] Cloke and coworkers synthesized the complex [μ:η^5,η^5-C_8H_4(1,4-$^i Pr_3Si)_2$]M_2 (M = Cr, Mo, Mn, Rh, Pd).[34−37] O'Hare and coworkers documented the synthesis of the permethylpentalene (Pn* = C_8Me_6) derivatives Li_2Pn*(TMEDA) and Pn*($SnMe_3$).[38,39] Recently, successful synthesis of bimetallic permethylpentalene complexes $Pn^*_2M_2$ (M = V, Cr, Mn, Co, and Ni) has been reported by Ashley et al.[40] They found that the complexes show structural, magnetic, and electrochemical behaviors markedly different from those found for their mononuclear cyclopentadienyl analogues.[40]

Here, we present the first *ab initio* study of 1D double metallocence nanowires, which are periodic units of the Pn_2M_2 complexes. We found that the 1D double metallocence nanowires can exhibit rich structural and electronic properties as well. All calculations were performed by a spin-polarized density-functional theory (DFT) method within the generalized gradient approximation (GGA) with the Perdew, Burke, and Ernzerhof (PBE) functional,[41] as implemented in the Vienna *ab initio* simulation package.[42,43] Interactions between ions and electrons are described by the frozen-core projector augmented wave method.[44,45] The plane-wave basis set cutoff energy is 500 eV, and a k-mesh of 1 × 1 × 15 within Monkhorst-Pack k-point scheme is adopted.[46] (Test calculations with a higher cutoff energy of 700 eV were also performed, and nearly the same results were obtained as shown in Figure S1 and Table S1). In the structural optimization, convergence of the Hellmann−Feynman forces (<0.01 eV/Å per atom) is achieved. Previous theoretical studies have shown that structural distortion may occur in 1D nanowires due to the Peierls transition.[47−49] To entail this possibility of structural distortion, we set up a supercell containing two Pn molecules and four metal atoms such that the initial structure is doubly repeated units of PnM_2. The tetragonal supercell has dimensions of 30 × 30 × c Å^3, where c is the periodic length in the axial direction. During the structural optimization, the periodic length c and positions of all atoms are relaxed.

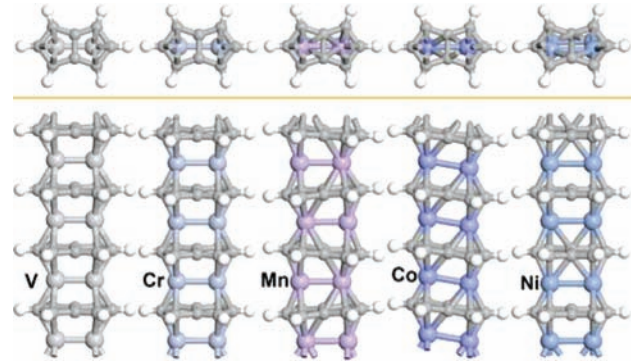

Figure 1. Top and front views of 1D PnM_2 (Pn = C_8H_6, M = V, Cr, Mn, Co, or Ni) nanowires. Two transition metal atoms are encompassed between two Pn planes; the 1D PnM_2 nanowires are periodically stacked Pn_2M_2 molecules in the direction normal to the Pn plane.

The predicted most stable structures of PnM_2 nanowires are displayed in Figure 1. The optimized structures are strongly dependent on the type of metal centers and electronic states of the nanowires (see Figure S2). The coordination characters of the metal and carbon atoms can change due to the interaction between two neighboring units, leading to different structures compared to their cluster analogues. In the *molecular complexes*, each V, Cr, or Mn atom is bonded to all five carbon atoms of a Cp ring, resulting in an η^5:η^5-coordination mode; each NI atom is bonded to three nonbridged carbon atoms, i.e., in an η^3:η^3-coordination mode, and each CO atom has an η^5:η^3-coordination mode with two faced Pn* fragments and the two neighboring Co atoms in the same layer show antisymmetric Co−C bonds.[40] On the other hand, in the 1D *nanowires*, each V or Cr atom is bonded to nonbridged C atoms, i.e., in the η^3:η^3-coordination mode. Co and Ni atoms still retain the same coordination modes as in the molecular complexes, but the Pn planes are tilted in the $PnCo_2$ nanowire while the Ni atoms are shifted (unlike their symmetric position in the molecular complex), resulting in metal−carbon bonding with bridged C atoms in the $PnNi_2$ nanowire. Another striking change can be seen in the $PnMn_2$ nanowire, where the two Mn atoms in the same layer are

10.1021/ja904912z CCC: $40.75

Table 1[a]

nanowire	c (Å)	GS	band gap (eV)	S_i (i = 1 to 4)	charge$_i$ (i = 1 to 4)	ΔE	M−M	E_b
PnV_2	7.402	AFM semicond	0.56 (indirect)	−1.12, 1.12, 1.12, −1.12	1.39, 1.39, 1.39, 1.39	0.061	**2.383**	**−5.24**
$PnCr_2$	7.727	AFM semicond	0.031 (direct)	−3.05, −3.05, 3.05, 3.05	1.15, 1.15, 1.14, 1.14	0.189	2.585	−3.20
$PnMn_2$	7.360	FM metal	/	1.51, 3.34, 3.33, 1.57	1.06, 1.05, 1.05, 1.06	−0.048	2.561	−3.18
$PnCo_2$	7.131	NM metal	/	0, 0, 0, 0	0.69, 0.69, 0.69, 0.69	/	2.567	−4.32
$PnNi_2$	7.404	NM semicond	0.027(indirect)	0, 0, 0, 0	0.60, 0.61, 0.61, 0.61	/	2.671	−4.14

[a] The lattice constant c in the axial direction, the ground state (GS), the electronic band gap, the local magnetic moment (S_i, i = 1 to 4, in μ_B unit) of metal atoms in one supercell, and the charge (Charge$_i$, i = 1 to 4 in e unit) of metal atoms in the supercell. The energy difference between the FM and AFM state (ΔE, in eV unit per metal atom, $\Delta E = E(\mathrm{FM}) - E(\mathrm{AFM})$), the average metal−metal distance (M−M, in Å unit), and the average binding energy per metal atom, defined by $E_b = [2E(\mathrm{Pn}) + 4E(\mathrm{M}) - E(\mathrm{Pn_2M_4})]/4$, where E($X$) is the energy of X (E_b, in eV unit).

bonded to C rings, i.e., in the η^5:η^5 and η^3:η^3-coordination mode, respectively. In the two nearest-neighbor layers, two Mn atoms switch their coordination modes. The Mn−C bond lengths are different in the η^5:η^5 and η^3:η^3-coordination modes, resulting in a weakly zigzag-like arrangement for the Pn planes in the $PnMn_2$ nanowire (Figure 1).

The intriguing zigzag-like structural distortion in the $PnMn_2$ nanowire may result from the Peierls instability, which might occur in a 1D nanowire if a partially filled energy band crosses the Fermi level at exactly the wavevector $k = \pi/2c$ (c is the lattice constant). The partially filled energy band could become unstable at low temperature due to strong electron−phonon interactions, resulting in dimerization along the axial direction in a nanowire.[47−49] Previous theoretical studies have shown that TMCp and TMBz nanowires are very stable without showing any Peierls transition.[29] Our electronic band-structure calculations with the smallest unit cell show that a half-filled band indeed crosses the Fermi level near the midpoint of the symmetry line of ΓZ for the $PnMn_2$ nanowire (see Figure S3). Hence, the coupling between the charge-density wave and the lattice vibration with a wavelength $2c$ can account for the structural distortion through the dimerization in a nanowire. In contrast, the band structure of PnV_2 does not exhibit such a half-filled band and thus its 1D wire structure is expected to be stable without structural distortion. As an independent test, we also started the structural optimization from a distorted structure (i.e. a structure with unparallel Pn layers) for all nanowires. All but the $PnMn_2$ nanowire recovered from the distorted configurations. Lastly, to ensure that the predicted structural distortion in the $PnMn_2$ nanowire is not due to the relatively small supercell, an independent calculation with a larger supercell (having *quadruply* repeated units of PnM_2) was performed, and the calculation confirms the occurrence of structural distortion in the ground state (Figure S4).

In Table 1, some structural, electronic, and magnetic properties of each PnM_2 nanowire are summarized. Specifically, the electronic structure calculations predict that the $PnMn_2$ and $PnCo_2$ nanowires are metallic, while other three nanowires are semiconducting with either direct or indirect band gaps, ranging from 0.027 to 0.56 eV. It is known that DFT-GGA tends to underestimate the band gap of semiconductors. The ground states of both PnV_2 and $PnCr_2$ nanowires are antiferromagnetic (AFM) with the energy difference between the ferromagnetic (FM) and AFM states being 61 and 189 meV per TM atom, respectively. The local magnetic moment is 1.12 and 3.05 μ_B for V and Cr atom, respectively. The $PnCo_2$ and $PnNi_2$ nanowires exhibit nonmagnetic (NM) ground states. Interestingly, the ground state of $PnMn_2$ nanowire is ferromagnetic. In the supercell, the local magnetic moments of the two Mn atoms in the η^3:η^3-coordination mode are 3.34 and 3.33 μ_B, and those of the two Mn atoms in the η^5:η^5-coordination mode are 1.51 and 1.57 μ_B, respectively. The energy difference between the FM and AFM state is ~ -48 meV per Mn atom. Note that we considered three initial AFM states, one like that (i.e. spin configuration) of PnV_2 [see colored spin density distribution shown in Figure 2a], another like that of $PnCr_2$ [see colored spin density distribution shown in Figure 2c], and the third with up−up local spin in one layer and down−down in the next layer. The AFM state like that of $PnCr_2$ is the most stable among the three. Note also that, for the molecular complexes, both Pn_2Co_2 and Pn_2Ni_2 are diamagnetic,[32,35] while the Pn_2Mn_2 is in the triplet ground state.[35]

In general, the magnetic behavior of PnM_2 nanowires is different from that of corresponding TM-Cp, TM-Bz, TM-Ant, or hybrid TM-CpBz nanowires. Many of the latter ones can be (quasi) half metallic.[22−31] The notable difference in the magnetic behavior is likely due to a relatively stronger M−M interaction in double metallocene nanowires. As shown in Table 1, the M−M distance in the double metallocene nanowires is <2.7 Å, much less than the distance between two nearest metal atoms in either $[TMBz]_\infty$ or $[TMCp]_\infty$ nanowires (usually >6 Å, along the axial direction).

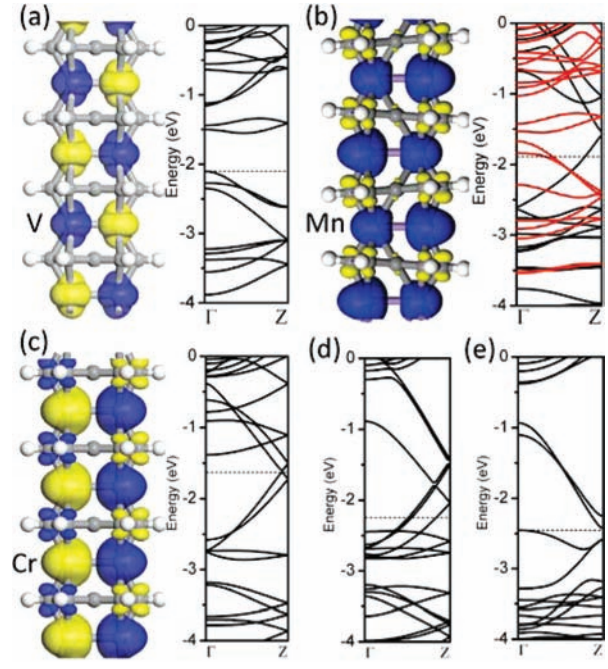

Figure 2. Spin charge density isosurfaces and electronic band structures along the Γ−Z line for (a) PnV_2, (b) $PnMn_2$, and (c) $PnCr_2$ nanowires, as well as the electronic band structures along the Γ−Z line for (d) $PnCo_2$ and (e) $PnNi_2$ nanowires. The value of the isosurface is 0.003 au. The electronic band structures for the major and minor spin states are shown with black and red lines, respectively. The dotted line denotes the Fermi energy level.

In Figure 2, the spin-charge density isosurfaces and electronic band structures of major and minor spin states of PnV_2, $PnCr_2$, and $PnMn_2$ nanowires are plotted. In the PnV_2 nanowire, the two V atoms in one layer favor the AFM coupling; the magnetic order of V atoms in the nearest-neighbor layer is opposite, which can be viewed as two parallel metallocene wires, each in the AFM ground state. In the $PnCr_2$

nanowire, the two Cr atoms in one layer still favor the AFM coupling, but the Cr atom in nearest-neighbor layers have the same magnetic order, equivalent to two parallel metallocene nanowires, each in the FM ground state. In contrast, in the $PnMn_2$ nanowire, all Mn atoms in one layer and neighboring layers favor the FM coupling. $PnCo_2$ and $PnNi_2$ nanowires have NM ground states without a net spin-charge distribution. Due to the interaction between two metal atoms in the same layer, the crystal field theory cannot be applied here for understanding the band structures near the Fermi level. For example, in the electronic band structures of the PnV_2 nanowire, the two lowest unoccupied bands are mainly contributed by $3d_{z^2}$ and $3d_{x^2}$ orbitals of V atoms, and the highest occupied state is mainly contributed by the $3d_{xz}$ orbital of V atoms and the $2p_z$ orbital of C atoms. In the $PnMn_2$ nanowire, the energy band crossing the Fermi level in the spin channel is mainly contributed by $3d_{x^2-y^2}$ and $3d_{z^2}$ orbitals of Mn atoms, and the two energy bands in the minor spin channel are mainly contributed by $3d_{xy}$, $3d_{x^2-y^2}$, and $3d_{z^2}$ orbitals, respectively.

Previous theoretical studies have suggested two mechanisms to explain the ferromagnetism in 1D organometallic sandwich nanowires, including the charge-transfer-based (CT) and double exchange (DE) mechanisms.[23,29,50−52] The ferromagnetism of Bz-based nanowires is due to the DE mechanism, and that of Cp-based wires is due to the CT mechanism. Like Cp, the Pn tends to capture two electrons to form a stable aromatic configuration with $4m + 2$ (where m is an integer) valence electrons (the Hückel rule), leading to an M_2^{2+} and Pn^{2-} alternative structure in a nanowire. The Bader charge analysis also confirms a charge transfer between metal atoms and Pn, as summarized in Table 1.[53−56] The anionic Pn rings are slightly polarized in the $PnMn_2$ and $PnCr_2$ nanowires. For example, the Pn ring in a $PnMn_2$ nanowire has a total magnetic moment of $-0.17\ \mu_B$. However, the partial density of states (PDOS) near the Fermi level (Figure S5) show that the ferromagnetism of the $PnMn_2$ nanowire stems mainly from the 3d orbitals of Mn atoms and, to much less extent, from the 2p orbitals of C atoms near the Fermi level. The strong coupling between Mn and Pn can be observed in the region below the Fermi level. Hence, the ferromagnetism of the $PnMn_2$ nanowire appears mainly due to the DE mechanism, but also, to a lesser extent, to the CT mechanism.

In conclusion, we have investigated properties of 1D double metallocene nanowires PnM_2 (M = V, Cr, Mn, Co, Ni) by a DFT method. We have shown that these 1D PnM_2 nanowires can exhibit rich structural, electronic, and magnetic properties. For example, the $PnMn_2$ nanowire is FM while other nanowires can be either AFM or NM. The $PnMn_2$ nanowire exhibits zigzag-like structural distortion that might result from the Peierls instability. The PnV_2 nanowire possesses the largest binding energy per atom (i.e., cohesive energy) and shortest metal−metal distance and is likely the most stable structure among the 1D double metallocene nanowires.

Acknowledgment. We thank Dr. Hongjun Xiang and Dr. Erjun Kan for their valued discussions. This work was supported by grants from the NSF (CHE-0427746, DMR-0820521) and Nebraska Research Initiative.

Supporting Information Available: Geometries of PnM_2 nanowires with different spin states; geometries and electronic band structures of PnM_2 nanowire calculated with the smallest unit cell; and the spin charge density distribution, electronic band structures, and projected density of states of PnM_2 nanowires. This material is available free of charge via the Internet at http://pubs.acs.org.

References

(1) Kealy, T. J.; Pauson, P. L. *Nature* **1951**, *168*, 1039–1040.
(2) Long, N. J. *Metallocenes: An Introduction to Sandwich Complexes*; Blackwell Science: Oxford, U.K., 1998.
(3) Weis, P.; Kemper, P. R.; Bowers, M. T. *J. Phys. Chem. A* **1997**, *101*, 8207–8213.
(4) Kurikawa, T.; Takeda, H.; Hirano, M.; Judai, K.; Arita, T.; Nagao, S.; Nakajima, A.; Kaya, K. *Organometallics.* **1999**, *18*, 1430–1438.
(5) Nakajima, A.; Kaya, K. A. *J. Phys. Chem. A* **2000**, *104*, 176–191.
(6) Hoshino, K.; Kurikawa, T.; Takeda, H.; Nakajima, A.; Kaya, K. *J. Phys. Chem.* **1995**, *99*, 3053–3055.
(7) Miyajima, K.; Nakajima, A.; Yabushita, S.; Knickelbein, M. B.; Kaya, K. *J. Am. Chem. Soc.* **2004**, *126*, 13202–13203.
(8) Miyajima, K.; Yabushita, S.; Knickelbein, M. B.; Nakajima, A. *J. Am. Chem. Soc.* **2007**, *129*, 8473–8480.
(9) Nagao, S.; Kato, A.; Nakajima, A. *J. Am. Chem. Soc.* **2000**, *122*, 4221–4222.
(10) Pandey, R.; Rao, B. K.; Jena, P.; Newsam, J. M. *Chem. Phys. Lett.* **2000**, *321*, 142–150.
(11) Pandey, R.; Rao, B. K.; Jena, P.; Blanco, M. A. *J. Am. Chem. Soc.* **2001**, *123*, 3799–3808.
(12) Wang, J.; Acioli, P. H.; Jellinek, J. *J. Am. Chem. Soc.* **2005**, *127*, 2812–2813.
(13) Wang, J.; Jellinek, J. *J. Phys. Chem. A* **2005**, *109*, 10180–10182.
(14) Kua, J.; Tomlin, K. M. *J. Phys. Chem.* **2006**, *110*, 11988–11994.
(15) Weng, H. M.; Ozaki, T.; Terakura, K. *J. Phys. Soc. Jpn.* **2008**, *77*, 014301.
(16) Xu, Z. F.; Xie, Y. M.; Feng, W. L.; Schaefer, H. F. *J. Phys. Chem. A* **2000**, *107*, 2716–2729.
(17) Zhang, X. Y.; Wang, J. L.; Gao, Y.; Zeng, X. C. *ACS Nano* **2008**, *3*, 537.
(18) Kurikawa, T.; Negishi, Y.; Satoshi, F. H.; Nagao, S.; Miyajima, K.; Nakajima, A.; Kaya, K. *J. Am. Chem. Soc.* **1998**, *120*, 11766–11772.
(19) Li, J.; Bursten, E. *J. Am. Chem. Soc.* **1998**, *120*, 11456–11466.
(20) Miyajima, K.; Knickelbein, M. B.; Nakajima, A. *J. Phys. Chem. A* **2008**, *112*, 366–375.
(21) Takegami, R.; Hosoya, N.; Suzumura, J.; Nakajima, A.; Yabushita, S. *J. Phys. Chem. A* **2005**, *109*, 2476–2486.
(22) Kandalam, A. K.; Rao, B. K.; Jena, P.; Pandey, R. *J. Chem. Phys.* **2004**, *120*, 10414.
(23) Xiang, H. J.; Yang, J. L.; Hou, J. G.; Zhu, Q. S. *J. Am. Chem. Soc.* **2006**, *128*, 2310–2314.
(24) Maslyuk, V. V.; Bagrets, A.; Meded, V.; Arnold, A.; Evers, F.; Brandbyge, M.; Bredow, T.; Mertig, I. *Phys. Rev. Lett.* **2006**, *97*, 097201.
(25) Koleini, M.; Paulsson, M.; Brandbyge, M. *Phys. Rev. Lett.* **2007**, *98*, 197202.
(26) Mokrousov, Y.; Atodiresei, N.; Bihlmayer, G.; Gel, S.; Blugel, S. *Nanotechnology* **2007**, *18*, 495402.
(27) Hosoya, N.; Takegami, R.; Suzumura, J.; Yada, K.; Koyasu, K.; Miyajima, K.; Mitsui, M.; Knickelbein, M. B.; Yabushita, S.; Nakajima, A. *J. Phys. Chem. A* **2005**, *109*, 9–12.
(28) Zhou, L.; Yang, S.; Ng, M.; Sullivan, M. B.; Tan, V. B. C.; Shen, L. *J. Am. Chem. Soc.* **2008**, *130*, 4023–4027.
(29) Shen, L.; Yang, S.-W.; Ng, M.-F.; Ligatchev, V.; Zhou, L.; Feng, Y. *J. Am. Chem. Soc.* **2008**, *130*, 13956–13960.
(30) Wang, L.; Cai, Z.; Wang, J.; Lu, J.; Luo, G.; Lai, L.; Zhou, J.; Qin, R.; Gao, Z.; Yu, D.; Li, G.; Mei, W. N.; Sanvito, S. *Nano Lett.* **2008**, *8*, 3640–3644.
(31) Mallajosyula, S. S.; Pati, S. K. *J. Phys. Chem. B* **2007**, *111*, 13877–13880.
(32) Katz, T. J.; Acton, N. *J. Am. Chem. Soc.* **1972**, *94*, 3281.
(33) Kaz, T. J.; Acton, N.; McGinnis, J. *J. Am. Chem. Soc.* **1972**, *94*, 6205.
(34) Kuchta, M. C.; Cloke, F. G. N.; Hitchcock, P. B. *Organometallics* **1998**, *17*, 1934.
(35) Cloke, F. G. N. *Pure Appl. Chem.* **2001**, *73*, 233.
(36) Balazs, G.; Cloke, F. G. N.; Harrison, A.; Hitchcock, P. B.; Green, J.; Summerscales, O. T. *Chem. Commun.* **2007**, 873.
(37) Balazs, G.; Cloke, F. G. N.; Gagliardi, L.; Green, J. C.; Harrison, A.; Hitchcock, P. B.; Shahi, A. R. M.; Summerscales, O. T. *Organometallics* **2008**, *27*, 2013.
(38) Ashley, A. E.; Cowley, A. R.; O'Hare, D. *Chem. Commun.* **2007**, 1512–1514.
(39) Ashley, A. E.; Cowley, A. R.; O'Hare, D. *Eur. J. Org. Chem.* **2007**, 2239–2242.
(40) Ashley, A. E.; Cooper, R. T.; Wildgoose, G. G.; Green, J. C.; O'Hare, D. *J. Am. Chem. Soc.* **2008**, *130*, 15662.
(41) Perdew, J. P.; Burke, K.; Ernzerhof, M. *Phys. Rev. Lett.* **1996**, *77*, 3865.
(42) (a) Kresse, G.; Furthmüller, J. *Phys. Rev. B* **1996**, *54*, 11169. (b) Kresse, G.; Furthmüller, J. *Comput. Mater. Sci.* **1996**, *6*, 15.
(43) Kresse, G.; Hafner, J. *Phys. Rev. B* **1993**, *47*, R558; *Phys. Rev. B* **1994**, *49*, 14251.
(44) Blöchl, P. E. *Phys. Rev. B* **1994**, *50*, 17953.
(45) Joubert, D.; Kresse, G. *Phys. Rev. B* **1999**, *59*, 1758.
(46) Pack, J. D.; Monkhorst, H. J. *Phys. Rev. B* **1976**, *13*, 5188.
(47) Peierls, R. E. *Quantum Theory of Solid*; Oxford University Press: London, 1955.
(48) Classen, R.; Sing, M.; Schwingenschlogl, U.; Blaha, P.; Dressel, M.; Jacobsen, C. S. *Phys, Rev. Lett.* **2002**, *88*, 096402.
(49) Choi, J. H.; Cho, J. H. *J. Am. Chem. Soc.* **2006**, *128*, 11340.
(50) Zener, C. *Phys. Rev.* **1951**, *82*, 403.
(51) Akai, H. *Phys. Rev. Lett.* **1998**, *81*, 3002.
(52) Sato, K.; Dederichs, P. H.; Katayama-Yoshida, H.; Kudrnovsky, J. *J. Phys.: Condens. Matter* **2004**, *16*, S5491.
(53) Bader, R. *Atoms in Molecules: A Quantum Theory*; Oxford University Press: New York, 1990.
(54) Henkelman, G.; Arnaldsson, A.; Jónsson, H. *Comput. Mater. Sci.* **2006**, *36*, 254.
(55) Sanville, E.; Kenny, S. D.; Smith, R.; Henkelman, G. *J. Comput. Chem.* **2007**, *28*, 899.
(56) Tang, W.; Sanville, E.; Henkelman, G. *J. Phys.: Condens. Matter* **2009**, *21*, 084204.

JA904912Z